TASK QUARTERLY 12 No 3, 273–287

# FAST ALGORITHMS FOR CALCULATIONS OF VISCOUS INCOMPRESSIBLE FLOWS USING THE ARTIFICIAL COMPRESSIBILITY METHOD

ZBIGNIEW KOSMA

*Institute of Applied Mechanics, Technical University of Radom,*
*Krasickiego 54, 26-600 Radom, Poland*
*zbigniew.kosma@pr.radom.pl*

(Received 28 April 2008)

**Abstract:** An artificial compressibility method is designed to simulate stationary two-and three-dimensional motions of a viscous incompressible fluid. A standard method of lines approach is applied in this contribution. A partial differential equation system is discretized in space by second-order finite-difference schemes on uniform computational grids, and the time-variable is preserved as continuous. Initial value problems for systems of ordinary differential equations for pressure and velocity components are computed using the Galerkin-Runge-Kutta method of third order. Some test calculations for laminar flows in square, cubic, triangular and semicircular cavities with one uniform moving wall and double bent channels are reported.

**Keywords:** Navier-Stokes equation, artificial compressibility, method of lines

## 1. Introduction

One of the early techniques proposed for solving the incompressible Navier-Stokes equations in a primitive variable form is the artificial compressibility method of Chorin [1]. In this method, the continuity equation is modified to include an artificial compressibility term which vanishes when a steady state solution is obtained. The introduced pseudo-time derivative of pressure directly couples pressure and velocity and changes the mathematical nature of the continuity equation from elliptic to hyperbolic. The system of hyperbolic-parabolic equations is well posed and the efficient numerical methods developed for compressible flows can be used to advance the system in artificial time.

Many realistic problems in low-speed aerodynamics and hydrodynamics can be addressed by the incompressible NS equations. In the last two decades, a considerable progress has been made in developing computational techniques for predicting flow fields in geometrically complex domains which are of practical interest in engineering and bioengineering applications. The accuracy and efficiency of the existing codes are now such that Computational Fluid Dynamics (CFD) is routinely used in the analysis

and improvement process of the existing designs and is a valuable tool in experimental programs and in the construction of new configurations. However, even with the use of the most powerful super-computers the CPU requirements for steady and unsteady computations are still very high.

Up to now many efforts have been made in the simulation of viscous flows by resolving the NS equations with the pseudocompressibility techniques [2–21]. It is usually various highly complicated finite difference schemes that are used for solving the obtained system of equations, the temporal derivative is approximated via generalized time differencing. In order to derive a linear algebraic system of equations, a linearization of viscous and inviscid fluxes has to be performed using Taylor series expansions.

To overcome the difficulties associated with the nonlinearity of NS equations a standard method of lines [22–25] approach is applied in this contribution. This technique offers an advantage over discretized methods in that the NS equations are linearized. A practical methodology for solving the steady NS equations in arbitrarily complex geometries is also proposed. Some complex geometrical configurations can be decomposed into a set of simpler subdomains. Each of them is designed to be easily discretized with a simple rectangular grid. The simplest approach for specifying boundary conditions near a curved or irregular boundary is to transfer all primitive variables from the boundary to the nearest grid knots. In this way the system of partial differential equation is discretized in space by second-order finite-difference schemes on uniform grids in physical domains with the same mesh sizes in each direction, to be then integrated in time. The initial-boundary value problem for the system of partial differential equations is then reduced to an initial value problem for the system of ordinary differential equations (mathematically parabolic) which can be solved numerically by any powerful ordinary differential equations solver. To simplify our analysis, this study focuses only on the frequently studied standard benchmark problems to validate the accuracy of the NS solvers because many approved experimental and numerical results have been reported in the literature.

## 2. Governing equations

With the pseudo-compressibility technique the non-dimensionalized governing equations in the Cartesian co-ordinate system become:

$$\left.\begin{aligned} \frac{\partial p}{\partial t}+\frac{1}{\beta}\frac{\partial V_j}{\partial x_j}&=0,\\ \frac{\partial V_i}{\partial t}+\frac{\partial}{\partial x_j}V_iV_j&=-\frac{\partial p}{\partial x_i}+\frac{1}{\mathrm{Re}}\frac{\partial}{\partial x_j}\frac{\partial}{\partial x_j}V_i, \end{aligned}\right\} \tag{1}$$

where $V_1$, $V_2$, $V_3$ are the velocity components, $p$ is the pressure, Re is the Reynolds number, and $\beta>0$ is the artificial compressibility parameter.

In the first component of the above equations, a time derivative of pressure is artificially added to the equation of continuity. However, since mass conservation is enforced only at the steady state, it is impossible to follow a physical time transient.

The artificial compressibility factor $\beta$ represents an artificial sound speed and affects the overall convergence rate. It is possible to increase the rate of convergence by selecting an optimum value of $\beta$, but this has to be done on a trial and error basis

for each problem. Through several computational experiments, the most convenient value of the pseudo-compressibility parameter $\beta$ has been found to be unity and this value will be kept constant in the entire domains of solution.

The physical boundary conditions for the equations of viscous flows (1) in primitive variables are specified as consisting of impermeability as well as of non-slip conditions at solid walls and of the requirement of assumed velocity profiles at channel inlets and outlets. The pressure is usually not given on the boundaries, but it can be determined from the momentum equations, and can be fixed in one point of the domain.

The original form of the artificial compressibility method has been developed for the steady-state problems [3, 5]. The first of equations (1) can be used to compute pressure fields. The method can also be extended to a time accurate formulation and there are numerous works in the literature describing various strategies for solving the unsteady flow problems, see *e.g.* [10, 13–16]. The time accurate solutions can be obtained by using a three-level formula to evaluate the time derivatives and adding a pseudo time-derivative in the momentum equations. The discretized momentum equations are solved for a divergence free velocity field at each successive time level.

## 3. Numerical approach

The proposed numerical technique, the method of lines, consists of converting the partial differential equations system (1) into an ordinary differential equation initial value problem by discretizing the spatial derivatives together with the boundary conditions for the first derivative of pressure via the classical finite difference approximations of second order [26]. This produces a system of ordinary differential equations of the general form:

$$\frac{d\boldsymbol{U}}{dt} = F(\boldsymbol{U}), \tag{2}$$

where $\boldsymbol{U} = [p, V_i]^T$ is the vector of dependent variables, and $F$ is a spatial differential operator.

The unknown values of pressure and velocity components in each inner knot of computational meshes are computed using the explicit Galerkin-Runge-Kutta method of third order [27]:

$$\begin{aligned} \boldsymbol{U}^{(1)} &= \boldsymbol{U}_n + \Delta t F(\boldsymbol{U}_n), \\ \boldsymbol{U}^{(2)} &= \frac{3}{4}\boldsymbol{U}_n + \frac{1}{4}\boldsymbol{U}^{(1)} + \frac{1}{4}\Delta t F(\boldsymbol{U}^{(1)}), \\ \boldsymbol{U}_{n+1} &= \frac{1}{3}\boldsymbol{U}_n + \frac{2}{3}\boldsymbol{U}^{(2)} + \frac{2}{3}\Delta t F(\boldsymbol{U}^{(2)}). \end{aligned} \tag{3}$$

Time advancement to a steady-state of viscous flows obtained with the third-order explicit Runge-Kutta-Galerkin method proved to be much more efficient than the backward-differentiation predictor-corrector method [28, 29].

## 4. Numerical simulation of various fluid flows

Numerical methods for incompressible Navier-Stokes equations are often verified for codes validation, on widely used benchmark problems; the driven square [30–55] and cubic cavity flows [38, 56–67]. The streamlines and comparisons between the results of the method of lines and those found in the literature are shown. Some other

numerical experiments with incompressible fluid flows are also considered: double bent channel flows as well as triangular and semi-circular driven cavity flows.

### *4.1. Square and cubic cavity problems*

Let us consider two-and three-dimensional driven cavity flows as drawn in Figure 1 as examples of the developed method which belong to the most popular test problems in the CFD community in spite of a velocity discontinuity at the cavities corners adjacent to the moving walls. A numerical simulation of the viscous incompressible fluid motion in cavities is not only technologically important but it is also of great scientific interest because it displays most fluid mechanical phenomena in simple geometrical settings.

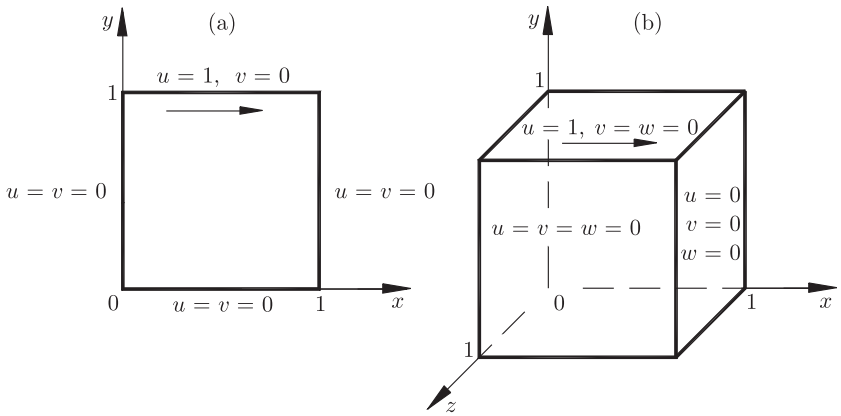


**Figure 1.** Geometry and boundary conditions of driven cavity problems: (a) square cavity flow, (b) cubic cavity flow

Computations in the square cavity on the uniform grid $200 \times 200$ have been performed for successive Reynolds numbers: $\mathrm{Re} = 10$, 100, 400, 1000, 3200, 5000 and 7500. The proposed algorithms seem to be quite promising as an incompressible Navier-Stokes solver for laminar flows, taking into account the fact that the transition from laminar to turbulent flows occurs about $\mathrm{Re} \approx 8000$.

First converged solutions for $\mathrm{Re} = 10$ with the assumption of $u, v = 0$ have been obtained to be then used as the initial conditions for the case of $\mathrm{Re} = 100$, and so forth. The time steps have been taken from the interval $5 \cdot 10^{-5} \leq \Delta t \leq 1 \cdot 10^{-3}$. The integration of the system of equations (2) has been terminated after arriving at the steady state, defined as:

$$\| \dot{\boldsymbol{U}}^{n+1} - \dot{\boldsymbol{U}}^{n} \| \leq \varepsilon = 1 \cdot 10^{-12}. \tag{4}$$

The obtained stream functions contours are shown in Figures 2 and 3. The numbers of iterations ranging from 30 000 to 100 000 were necessary to achieve the steady state solutions. Figures 4 and 5 present the computed profiles, and concern the $u$-velocity component on the cavity's vertical centreline, the $v$-velocity component along the cavity's horizontal centreline and their comparison with the corresponding data from [30].

By using the presented algorithm, the computations in the cubic cavity have been undertaken on a uniform $100 \times 100 \times 100$ grid. The numerical simulations have

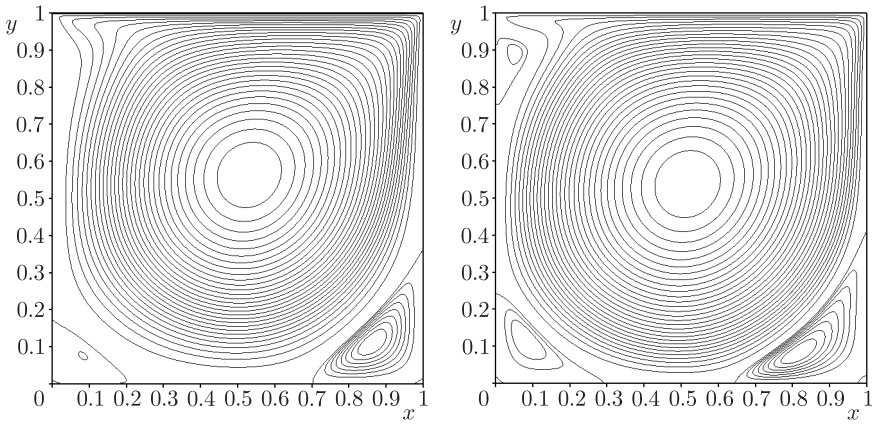


**Figure 2.** Square cavity: stream-function contours for Re = 1000 (left) and 3200 (right), $200 \times 200$ grid

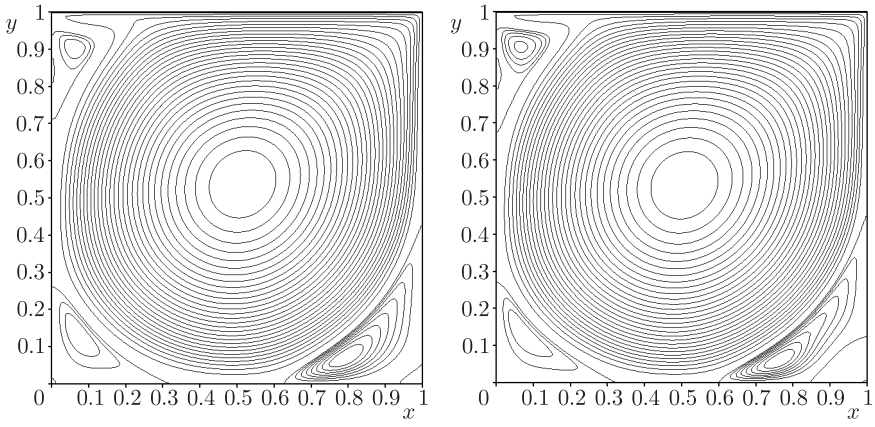


**Figure 3.** Square cavity: stream-function contours for Re = 5000 (left) and 7500 (right), $200 \times 200$ grid

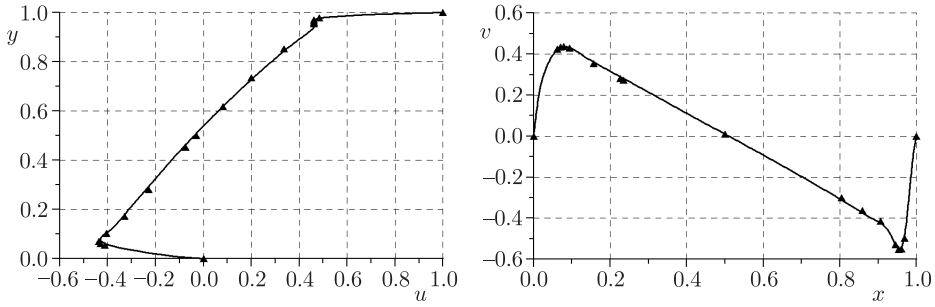


**Figure 4.** Distributions of $x$- and $y$-components of velocity on 2D-cavity centrelines at Re = 5000, $200 \times 200$ grid; solid line – the presented method, triangles – Ghia *et al.*, $x = 0.5$ (left), $y = 0.5$ (right)

been conducted with $\Delta t = 1 \cdot 10^{-3}$ for the Reynolds numbers: Re = 10, 100, 400 and 1000. The solutions have been qualified as steady for the relative error (4) between two time steps. It takes approximately 50 000 – 80 000 time steps to converge. The

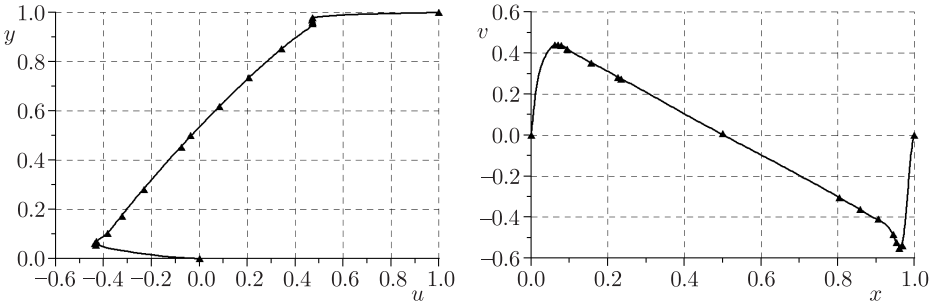


**Figure 5.** Distributions of $x$- and $y$-components of velocity on 2D-cavity centrelines at $\mathrm{Re} = 7500$, $200 \times 200$ grid; solid line – the presented method, triangles – Ghia *et al.*, $x = 0.5$ (left), $y = 0.5$ (right)

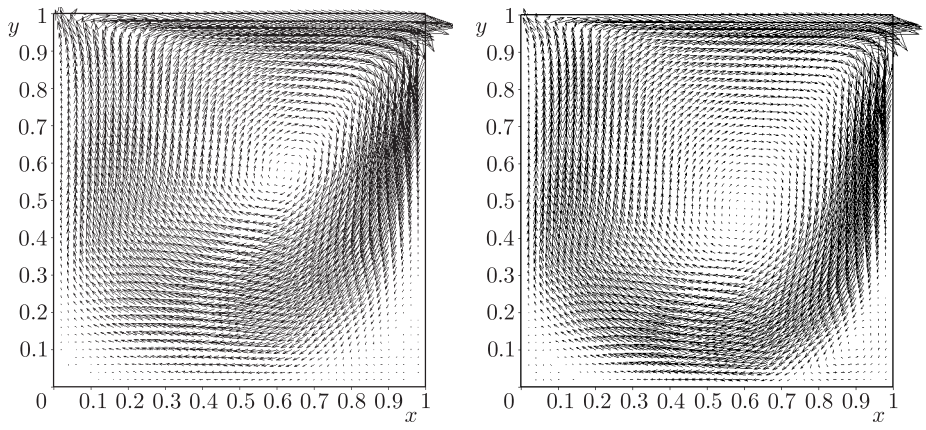


**Figure 6.** Cubic cavity: velocity vectors for $\mathrm{Re} = 400$ (left) and 1000 (right) on the $z = 0.5$ plane, $100 \times 100 \times 100$ grid

velocity vectors of the steady state solutions on the symmetry plane ($z = 0.5$) for the Reynolds numbers $\mathrm{Re} = 400$ and 1000 are presented in Figure 6. For the purpose of validation, Figures 7 and 8 show the plots of velocity profiles $u$ and $v$ along central axes on the $z = 0.5$ plane and their comparison to the results of Shu *et al.* [63].

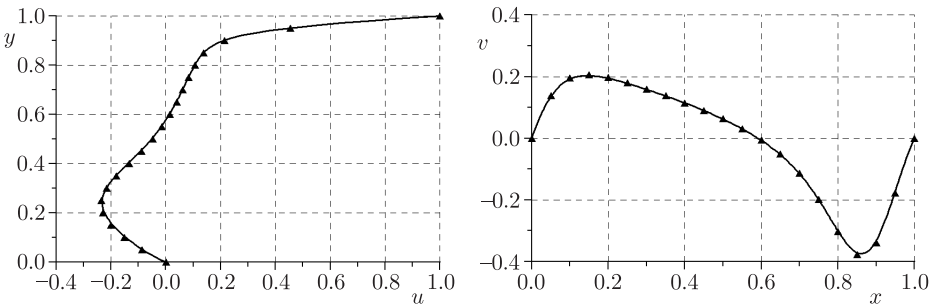


**Figure 7.** Velocity profiles for $u$ and $v$ on the centrelines of the 3D-cavity on $z = 0.5$ plane, $\mathrm{Re} = 400$, $100 \times 100 \times 100$ grid; solid line – the presented method, triangles – Shu *et al.*, $x = 0.5$ (left), $y = 0.5$ (right)

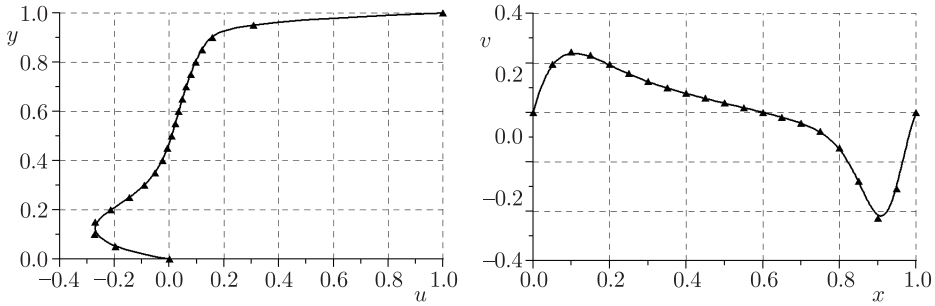


**Figure 8.** Velocity profiles for $u$ and $v$ on 3D-cavity centrelines on $z=0.5$ plane, $\mathrm{Re}=1000$, $100\times100\times100$ grid; solid line – the presented method, triangles – Shu *et al.*, $x=0.5$ (left), $y=0.5$ (right)

### *4.2. Flow in double bent channels*

The aim of this test case [47, 68–70] is to demonstrate the effectiveness of the presented numerical algorithms and artificial compressibility formulation of the Navier-Stokes equations in geometrical domains bounded by contours consisting of finite numbers of rectilinear segments, parallel to the axes of the co-ordinate system. An example of the flow in double bent channels with two concave corners is considered. Figure 9 shows the geometry in which all the channels have the height of $H=1$, the upper and lower channels lengths have been maintained in all configurations by setting $L_1=2$ and $L_3=9$ with the channel step ratio of $H\le L_2\le 5H$.

A parabolic velocity profile is imposed as the boundary conditions at the upper channel inlet and a zero pressure gradient is assumed. The non-slip condition on the solid walls is prescribed for the velocity components and the pressure is computed with the known normal pressure gradients from the Navier-Stokes equations. The outlet velocity field in the lower channel is also specified as a parallel flow with a parabolic velocity profile and the pressure is set as equal to a constant value.

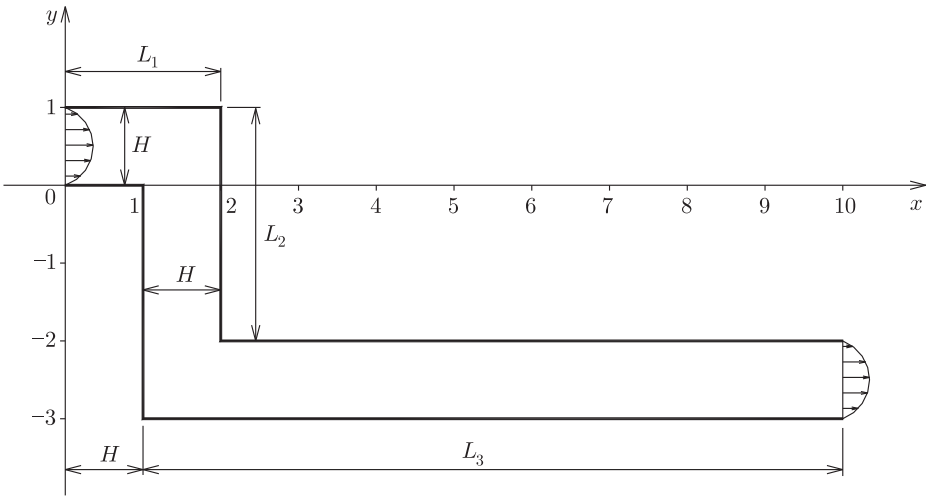


**Figure 9.** Geometry for double bent channels

The applied methodology consists in decomposition of the computational domain into a set of rectangles. After the domain decomposition has been completed, the relative location of the various rectangles and the manner in which they are connected with each other need to be determined, the sets of rectangular coordinates determine every rectangle separately. The solution to this problem, which is collectively referred to as grid connectivity, is trivial even when a large number of adjacent rectangles is employed.

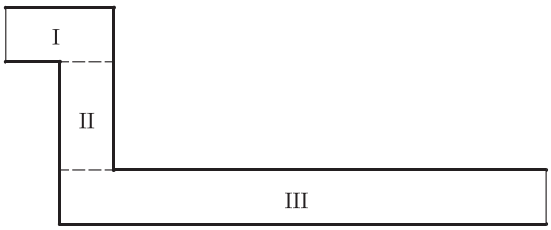


**Figure 10.** Schematic of a double bent channel domain with three adjacent rectangles

Using the developed algorithm, calculations for double bent channels flows have been performed for $\mathrm{Re} \leq 200$ on two ($L_2 = 1$): $100 \times 50$, $50L \times 50$ or three ($L_2 > 1$): $100 \times 50$, $50 \times 50L$ and $50L \times 50$ uniform grids (Figure 10) for channels lengths $1 \leq L \leq 9$. The original problem is solved on each successive rectangle for the known tentative values of velocity components and pressure separately, and the values on the adjacent boundaries are exchanged. The calculations have been made with $\Delta t = 1 \cdot 10^{-3}$ and 10 000–90 000 time steps on each grid have been necessary to get convergent solutions. Figures 11–13 show the computed stream-function contours for three channel step ratios $L_2 = 1,3,5$, respectively.

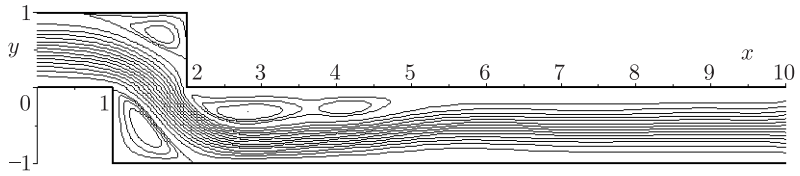


**Figure 11.** Double bent channel: stream-function contours, $\mathrm{Re} = 200$, $L_2 = 1$

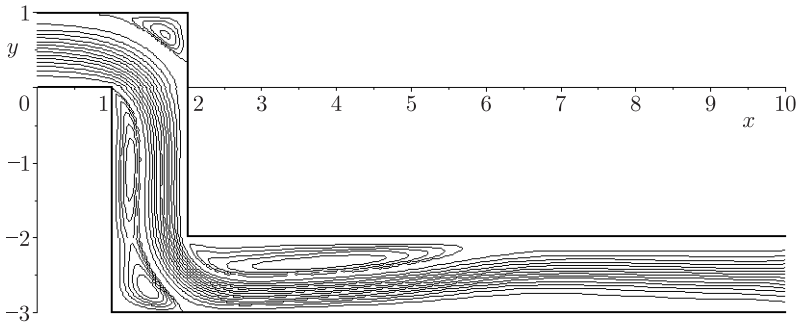


**Figure 12.** Double bent channel: stream-function contours, $\mathrm{Re} = 200$, $L_2 = 3$

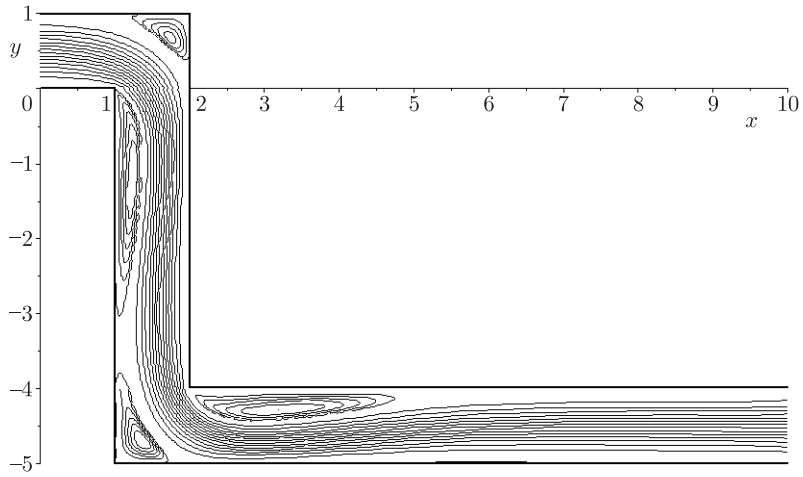


**Figure 13.** Double bent channel: stream-function contours, $\mathrm{Re} = 200$, $L_2 = 5$

### *4.3. Triangular and semicircular cavity problems*

In this section the artificial compressibility method in conjunction with the method of lines is applied to calculate laminar flows in complex geometrical configurations. The driven flows in triangular and semicircular cavities are considered [71–75]. The number of publications dedicated to these wall-driven incompressible viscous flow problems is not as large as in the case of wall-driven square and cubic cavities problems, for which various solution methods have been compared. The geometry of triangular and semicircular cavities with a co-ordinate system is shown in Figures 14a and 14b. As in the case of square and cubic cavity problems, a unit velocity is prescribed on the top boundary, while the no-slip boundary conditions are imposed on the remaining boundaries.

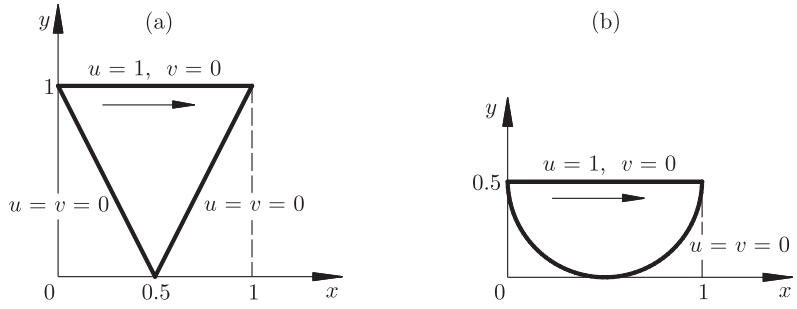


**Figure 14.** Geometry and boundary conditions of driven cavity problems: (a) triangular cavity flow, (b) semicircular cavity flow

Uniform grids are used to discretize the domains of solutions. The left and right boundaries of the triangle and the curvilinear edge of the semicircle are approximated by rectilinear edges or diagonals joining consecutive vertices of meshes, nearest to the sidelines boundaries of the cavities (Figure 15). The following two matrices can be useful to construct the resulting computer codes:

– a two-dimensional matrix with logical elements to the identification mesh knots which determine step-shaped lines approximating the unmoving boundaries of the cavities,
– a one-dimensional matrix with integer elements containing numbers of the first inner knots on vertical grid lines.

The systems of semi-discrete (discrete in space, continuous in time) ordinary differential equations (2) can be thus obtained in all the nodes of the assumed uniform computational grids situated inside the boundaries of cavities.

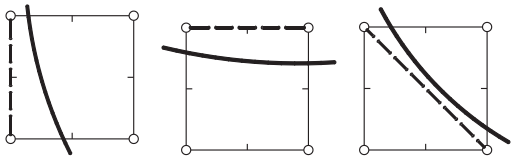

**Figure 15.** Some curved boundary line approximations

The flow in the triangular cavity has been simulated for Reynolds numbers of $\mathrm{Re} \leq 5000$ with the mesh size $h = 1/300$, the flow in the semicircular cavity – for Reynolds numbers of $\mathrm{Re} \leq 6600$ with the mesh size $h = 1/250$. The computations have been done with the time step $\Delta t = 1 \cdot 10^{-4}$ until the criterion (4) for convergence has been satisfied. The obtained velocity vectors and stream function contours for some Reynolds numbers are presented in Figures 16–22.

## 5. Remarks and conclusions

A very efficient and accurate numerical approach based on the artificial compressibility and lines methods is developed in this work for predicting steady laminar flows at high Reynolds numbers. The time integration has been obtained by the third-stage Galerkin-Runge-Kutta scheme. The details of the numerical procedure employed to solve the governing equations are presented, and a brief description of the applied strategy is provided. The proposed algorithms have proved to be very effective for the demanded time of calculations required for steady-state computations, they offer a significant acceleration of computations in comparison with the previous algorithms [28, 29], and the calculation time of the same problem solutions obtained by using the Fluent solver.

Simulations of 2D and 3D lid-driven cavity flows as well as flows in double bent channels and triangular and semicircular cavities have been performed for various Reynolds numbers. The steady-state numerical results for these flows are compared to the results reported in the literature. It has been found that the proposed approach yields the same velocity profiles along the vertical and horizontal lines on the midplane of square and cubic cavities and the same velocity and stream-function fields in the other regarded domains.

In the past decades, much progress has been made in developing computational techniques for predicting flow fields in complex geometries. The widely used methods have included finite element and finite volume methods due to their ability to analyze the domains of an arbitrary shape. Although automatic grid generation is usually a very effective solution, the mesh is difficult to be fully generated in many engineering

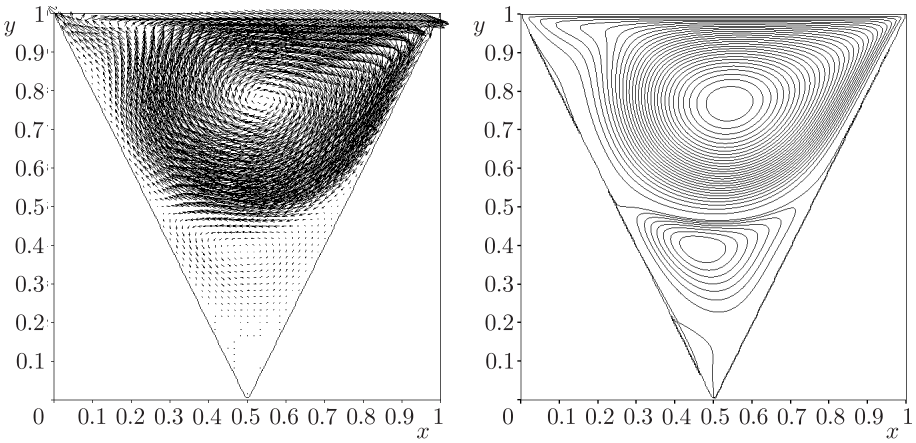


**Figure 16.** Triangular cavity: velocity vectors and stream-function contours for $\mathrm{Re} = 1000$, mesh size $h = 1/300$

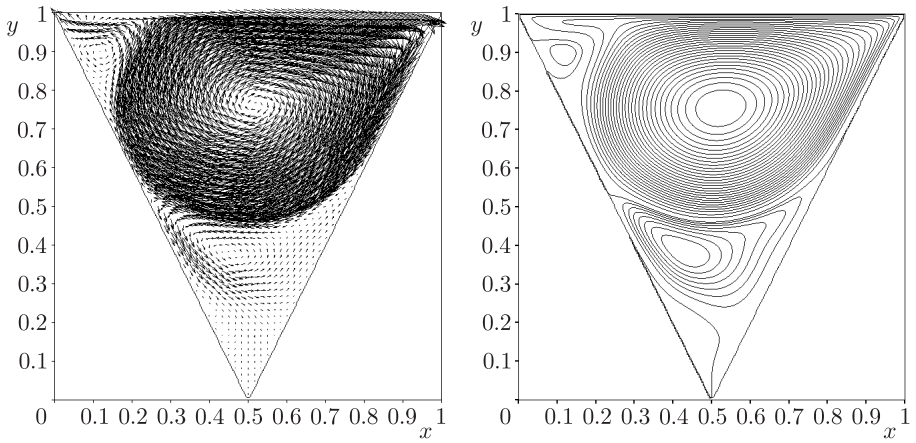


**Figure 17.** Triangular cavity: velocity vectors and stream-function contours for $\mathrm{Re} = 3000$, mesh size $h = 1/300$

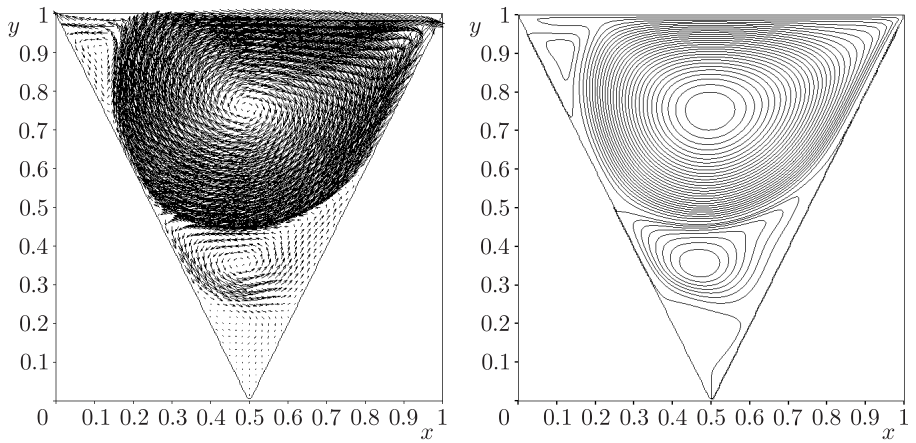


**Figure 18.** Triangular cavity: velocity vectors and stream-function contours for $\mathrm{Re} = 5000$, mesh size $h = 1/300$

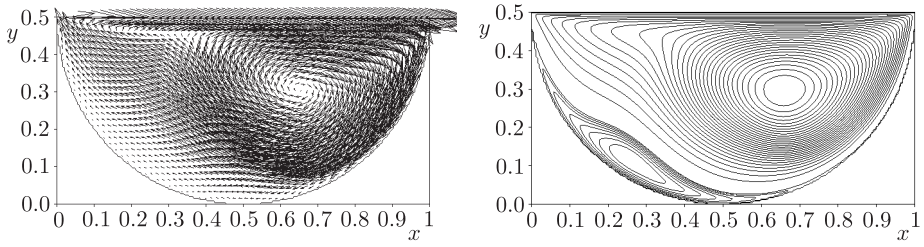


**Figure 19.** Semicircular cavity: velocity vectors and stream-function contours for $\mathrm{Re} = 1000$, mesh size $h = 1/250$

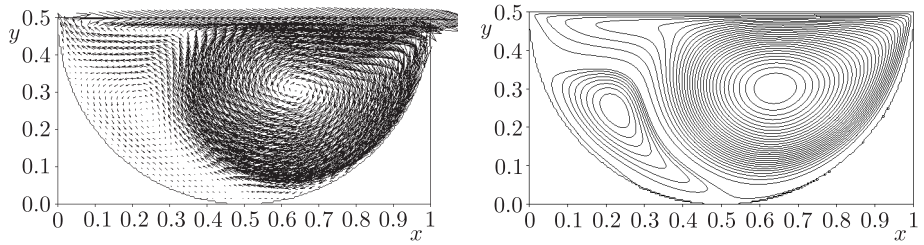


**Figure 20.** Semicircular cavity: velocity vectors and stream-function contours for $\mathrm{Re} = 2000$, mesh size $h = 1/250$

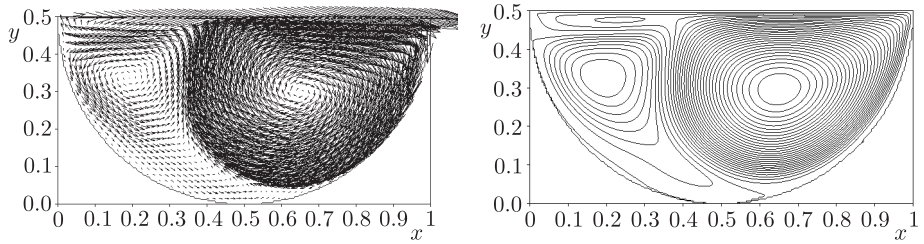


**Figure 21.** Semicircular cavity: velocity vectors and stream-function contours for $\mathrm{Re} = 4000$, mesh size $h = 1/250$

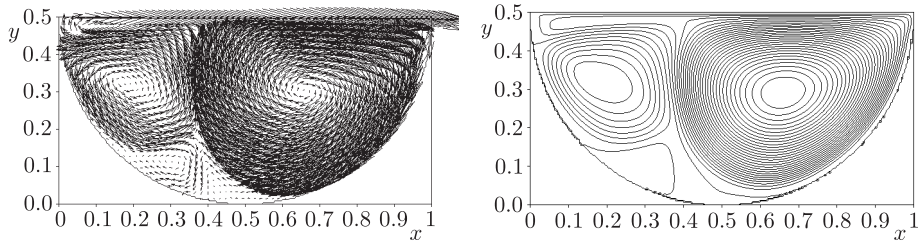


**Figure 22.** Semicircular cavity: velocity vectors and stream-function contours for $\mathrm{Re} = 6600$, mesh size $h = 1/250$

problems, and pre-specified connectivity between the computational nodes or grid points is required. In order to avoid the troublesome processing of mesh generation, a number of meshless methods have been proposed in which the analysis domain is discretized without employing any mesh or elements. Mesh-free methods usually require node generation instead of mesh generation. Functions and their derivatives at one central node are approximated entirely from the information of a set of scattered

nodes within its local support. From the point of view of computational efforts, node generation is considered to be an easier and faster job, compared to the former one. Rather than calling these methods an alternative for meshbased methods, they may be labeled as specific tools because the price to pay is a relatively high computational burden associated with the use of these methods.

An alternative and practical methodology for solving the Navier-Stokes equations in arbitrarily complex geometries using Cartesian meshes which have numerous inherent advantages is proposed in the paper. These include simple and efficient field mesh generation, superior implementation of discretization schemes, minimal associated phase errors, and absence of any issues associated with mesh skewness and distortion. However, an obvious difficulty with the Cartesian approach is the implementation of solid wall boundary conditions, and their approximation error strongly depends on the mesh size value. The scheme presented in this paper is spatially isotropic (which is important for general applications) and shows good stability and accuracy in the test problems solved. The schemes have been presented and tested for two-dimensional solutions, but in principle the given procedure can also be developed directly for three-dimensional analyses. Of course, further studies of the scheme, for two-dimensional solutions are needed to include the numerical effectiveness. The potential of the domain decomposition method onto a set of rectangles with rectilinear or curved sides is demonstrated as a technique for simulating complex engineering flows. Besides, near curved or irregular boundaries unequal mesh spacings and special rules may be considered. The research in this direction is in progress. Because the tentative velocity and pressure fields are given, the numerical calculations in each subdomain can be done separately. The extension of the algorithms provides a tool for studying problems in many engineering applications that involve complex geometries and flows.

## *References*


[1] Chorin A J 1967 *J. Comput. Phys.* **2** 12
[2] Liu H and Ikehata M 1994 *Int. J. Numer. Meth. Fluids* **19** 395
[3] Pentaris A, Nikolados K and Tsangaris S 1994 *Int. J. Numer. Meth. Fluids* **19** 1013
[4] Anderson W K, Rausch R D and Bonhaus D L 1996 *J. Comput. Phys.* **128** 391
[5] Pappou T and Tsangaris S 1997 *Int. J. Numer. Meth. Fluids* **25** 523
[6] Liu C, Zheng X and Sung C H 1998 *J. Comput. Phys.* **139** 35
[7] Dridakis D, Iliev O P and Vassileva D P 1998 *J. Comput. Phys.* **146** 301
[8] Yuan L 2002 *J. Comput. Phys.* **177** 134
[9] He X, Doolen G D and Clark T 2002 *J. Comput. Phys.* **179** 439
[10] Tang H S, Jones S C and Sotiropoulos F 2003 *J. Comput. Phys.* **191** 567
[11] Tai C H and Zhao Y 2003 *J. Comput. Phys.* **192** 277
[12] Mendez B and Velazquez A 2004 *Comput. Meth. Appl. Mech. Engrg.* **193** 825
[13] Ekaterinaris J A 2004 *Int. J. Numer. Meth. Fluids* **45** 1187
[14] Kallinderis Y and Ahn H T 2005 *J. Comput. Phys.* **210** 75
[15] Shapiro E and Drikakis D 2005 *J. Comput. Phys.* **210** 584
[16] Shapiro E and Drikakis D 2005 *J. Comput. Phys.* **210** 608
[17] Nithiarasu P and Liu C-B 2006 *Comput. Meth. Appl. Mech. Engrg.* **195** 2961
[18] Lin P T, Baker T J, Martinelli L and Jameson A 2006 *Int. J. Numer. Meth. Fluids* **50** 199
[19] Lee J W, Teubner M D, Nixon J B and Gill P M 2006 *Int. J. Numer. Meth. Fluids* **51** 617
[20] Nithiarasu P and Zienkiewicz O C 2006 *Comput. Meth. Appl. Mech. Engrg.* **195** 5537
[21] Tang H S and Sotiropoulus F 2007 *Comput. Fluids* **36** 974

[22] Oymak O and Selçuk N 1996 *Int. J. Numer. Meth. Fluids* **23** 455
[23] Šolin P and Segeth K 2003 *Int. J. Numer. Meth. Fluids* **41** 519
[24] Tang H and Warnecke G 2005 *Comput. Fluids* **34** 375
[25] 2005 *J. Comput. Appl. Math.* **183** 241 (Special Issue on the Method of Lines)
[26] Kosma Z 2008 *Numerical Methods for Engineering Applications, 5$^{th}$ Edition*, Technical University of Radom Publishing (in Polish)
[27] Cockburn B and Shu C-W 1998 *J. Comput. Phys.* **141** 199
[28] Kosma Z and Noga B 2006 *Chemical Process Engrg.* **27** 761
[29] Kosma Z 2007 *Numerical simulation of viscous fluid motions using the artificial compressibility method*, Monography of Technical University of Radom (in Polish)
[30] Ghia U, Ghia K N and Shin C T 1982 *J. Comput. Phys.* **48** 387
[31] Kim J and Moin P 1985 *J. Comput. Phys.* **59** 308
[32] Tanahashi T and Okanaga H 1990 *Int. J. Numer. Meth. Fluids* **11** 479
[33] Kovacs A and Kawahara M 1991 *Int. J. Numer. Meth. Fluids* **13** 403
[34] Ren G and Utnes T 1993 *Int. J. Numer. Meth. Fluids* **17** 349
[35] Li M, Tang T and Fornberg B 1995 *Int. J. Numer. Meth. Fluids* **20** 1137
[36] Barragy E and Carey G F 1997 *Comput. Fluids* **26** 453
[37] Botella O and Peyret R 1998 *Comput. Fluids* **27** 421
[38] Shankar P N and Deshpande M D 2000 *Annu. Rev. Fluid Mech.* **32** 93
[39] Aydin M and Fenner R T 2001 *Int. J. Numer. Meth. Fluids* **37** 45
[40] Barton I E, Markham-Smith D and Bressloff N 2002 *Int. J. Numer. Meth. Fluids* **38** 747
[41] Peng Y-F, Shiau Y-H and Hwang R R 2003 *Comput. Fluids* **32** 337
[42] Mai-Duy N and Tran-Cong T 2003 *Int. J. Numer. Meth. Fluids* **41** 743
[43] Sahin M and Owens R G 2003 *Int. J. Numer. Meth. Fluids* **42** 57
[44] Sahin M and Owens R G 2003 *Int. J. Numer. Meth. Fluids* **42** 79
[45] Piller M and Stalio E 2004 *J. Comput. Phys.* **197** 299
[46] Gravemeier V, Wall W A and Ramm E 2004 *Comput. Meth. Appl. Mech. Engrg.* **193** 1323
[47] Ramšak M and Škerget L 2004 *Int. J. Numer. Meth. Fluids* **46** 815
[48] Wu Y and Liao S 2005 *Int. J. Numer. Meth. Fluids* **47** 185
[49] Erturk E, Corke T C and Gökçöl C 2005 *Int. J. Numer. Meth. Fluids* **48** 747
[50] Brüger A, Gustafsson B, Lötstedt P and Nilsson J 2005 *J. Comput. Phys.* **203** 49
[51] Abide S and Viazzo S 2005 *J. Comput. Phys.* **206** 252
[52] Gelhard T, Lube G, Olshanskii M A and Starcke J-H S 2005 *J. Comput. Appl. Math.* **177** 243
[53] Bruneau C-H and Saad M 2006 *Comput. Fluids* **35** 326
[54] Masud A and Khurram R A 2006 *Comput. Meth. Appl. Mech. Engrg.* **195** 1750
[55] Prabhakar V and Reddy J N 2006 *J. Comput. Phys.* **215** 274
[56] Guy G and Stella F 1993 *J. Comput. Phys.* **106** 286
[57] Jiang B-N, Lin T L and Povinelli L A 1994 *Comput. Meth. Appl. Mech. Engrg.* **114** 213
[58] Tang L Q, Cheng T and Tsang T T H 1995 *Int. J. Numer. Meth. Fluids* **21** 413
[59] Dridakis D, Iliev O P and Vassileva D P 1998 *J. Comput. Phys.* **146** 301
[60] Paisley M F 1999 *Int. J. Numer. Meth. Fluids* **30** 441
[61] Liu C H 2001 *Int. J. Numer. Meth. Fluids* **35** 533
[62] Sheu T W H and Tsai S F 2002 *Comput. Fluids* **31** 911
[63] Shu C, Wang L and Chew Y T 2003 *Int. J. Numer. Meth. Fluids* **43** 345
[64] Nithiarasu P, Mathur J S, Weatherill N P and Morgan K 2004 *Int. J. Numer. Meth. Fluids* **44** 1207
[65] Lo D C, Murugesan K and Young D L 2005 *Int. J. Numer. Meth. Fluids* **47** 1469
[66] Albensoeder S and Kuhlmann H C 2005 *J. Comput. Phys.* **206** 536
[67] Ding H, Shu C, Yeo K S and Xu D 2006 *Comput. Meth. Appl. Mech. Engrg.* **195** 516
[68] Tulapurkara E G, Lakshmana Gowda B H and Balachandran N 1988 *J. Fluid Mech.* **190** 179
[69] Hwang Y-H 1994 *J. Comput. Phys.* **110** 134
[70] Bathe K-J and Zhang H 2002 *J. Comput. Phys.* **80** 1267
[71] Jyotsna R and Vanka S P 1995 *J. Comput. Phys.* **122** 107

[72] Lai M-J and Wenston P 2004 *Comput. Fluids* **33** 1047
[73] Kohno H and Bathe K-J 2006 *Int. J. Numer. Meth. Fluids* **51** 673
[74] Glowinski R, Guidoboni G and Pan T-W 2006 *J. Comput. Phys.* **216** 76
[75] Pontaza J P 2007 *J. Comput. Phys.* **221** 649